Copper(II) Complexes of Substituted Salicylaldehyde Dibenzyl Semicarbazones: Synthesis, Cytotoxicity and Interaction with Quadruplex DNA

Siti Munira Haidad Ali[a], Yaw-Kai Yan[a,*], Peter P. F. Lee[a], Kenny Zhi Xiang Khong[a], Mahasin Alam Sk[b], Kok Hwa Lim[b], Beata Klejevskaja[c], Ramon Vilar[c],

[a] *Natural Sciences & Science Education, National Institute of Education, Nanyang Technological University, 1 Nanyang Walk, Singapore 637616*
[b] *Division of Chemical & Biomolecular Engineering, School of Chemical & Biomedical Engineering, Nanyang Technological University, Singapore*
[c] *Department of Chemistry, Imperial College London, London SW7 2AZ, UK*

Abstract

A series of substituted salicylaldehyde dibenzyl semicarbazones [$RC_6H_3(OH)CH{=}N{-}NHCON(CH_2Ph)_2$] and their copper(II) complexes were synthesized and characterized. The chloridocopper(II) complexes of the 4-OH and 5-OH substituted ligands (complexes **9** and **7**) show modest affinity and good selectivity (over duplex DNA) for the quadruplex formed from the 22AG human telomeric (HTelo) DNA sequence. Substitution of the chlorido ligands of these two complexes with pyridine yielded derivatives (**7-py** and **9-py**) with increased affinity for HTelo. These derivatives also show good selectivity for HTelo over calf-thymus DNA (170- and 211-fold, respectively). The X-ray crystal structures of **9** and **9-py** were determined. Molecular docking studies based on these structures show that the complexes stack on the 5′-end of the HTelo quadruplex, with the hydroxyl group forming a hydrogen bond with a guanine residue. Complexes **7**, **9**, **7-py** and **9-py** display significant cytotoxicity against MOLT-4 human leukaemia cells. Interestingly, they have low to negligible cytotoxicity against the non-cancerous IMR-90 human fibroblasts.

Keywords: copper(II); semicarbazones; quadruplex DNA; cytotoxicity; molecular docking.

* Correspondence author. Email: yawkai.yan@nie.edu.sg; Fax: 65-6896-9414; Tel: 65-6790-3813

1 Introduction

G-quadruplex DNA structures are four-stranded, guanine-rich DNA structures containing coplanar square quartets of guanine residues held together by hydrogen bonding. [1-3] Such guanine-rich sequences can exist in telomeres and in promoter regions of some oncogenes in the human genome.[4] The activity of telomerase, an enzyme that is crucial for the immortalization of cancerous cells,[5] can be inhibited if the single stranded telomeric DNA is folded into a quadruplex structure.[6] Formation of quadruplex structures in the promoter regions of oncogenes like *c-myc* and *c-kit* has been proposed to regulate the transcription of these genes.[7-11] Molecules that bind to, and stabilize, quadruplex DNA are therefore of interest as potential anticancer agents.[12-20]

We have reported a square planar copper(II) complex of salicylaldehyde *N,N*-dibenzyl semicarbazone (**1**, Scheme 1) that is strongly cytotoxic against a range of human cancer cell lines.[21] This complex induces apoptosis on MOLT-4 (human leukaemia) cells and downregulates proteins that are associated with transcription, translation, protein folding, glucose metabolism, signal transduction and mitosis.[21] It also intercalates with duplex DNA and cleaves it via the generation of reactive oxygen species.[22] With its square planar geometry and aromatic ligand, complex **1** potentially has the ability for quadruplex binding. Hence, we decided to determine the binding strength of **1** and its derivatives (Scheme 1) for quadruplex DNA, and their selectivity for quadruplex over duplex DNA. The results are reported in this paper, together with the cytotoxicity of these compounds towards MOLT-4 human leukaemia cells and IMR-90 human fibroblasts (non-cancerous).

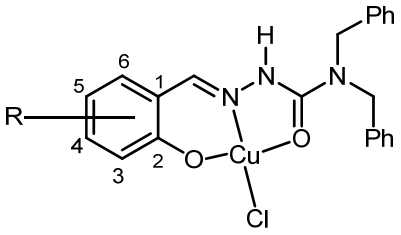

Complex	R
1	5-H
2	5-Cl
3	5-Br
4	5-NO_2
5	5-OMe
7	5-OH
8	3-OH
9	4-OH
10	6-OH

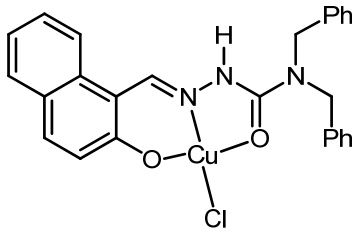

6

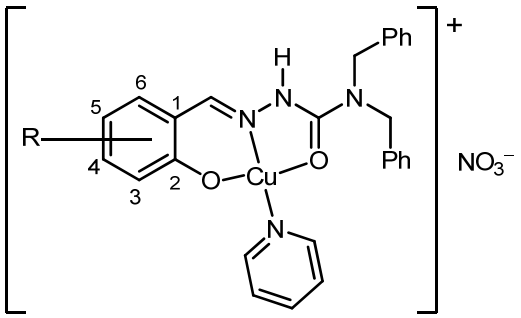

7-py (R = 5-OH) , **9-py** (R = 4-OH)

Scheme 1

2 Experimental

2.1 Materials and apparatus

Chemical reagents, unless otherwise stated, were obtained commercially and were used as received without any pre-treatment. All chemical reactions involving air- and/or moisture sensitive compounds were performed under nitrogen atmosphere using standard Schlenk techniques. Solvents used for the reactions were of reagent grade and toluene, dichloromethane and diethyl ether were distilled under nitrogen and vacuum-degassed before use. Elemental analyses (C, H and N) were performed using a Elementar Vario Micro Cube elemental analyzer. Solid-state infrared spectra (KBr pellet) were recorded using a Perkin-Elmer Spectrum 100 FTIR spectrometer of operating region 4000 to 400 cm^{-1}. Proton NMR spectra were recorded in $(CD_3)_2SO$ on a Bruker DRX400 spectrometer at room temperature at 400 MHz. Chemical shifts are quoted in ppm downfield of internal tetramethylsilane.

Fluorescence spectra were recorded using a Perkin-Elmer L50 photoluminescence spectrometer, while UV-vis spectra were recorded on a Perkin-Elmer 25 UV-vis spectrophotometer.

All oligonucleotides used were purchased from either AITBiotech (Singapore) or Eurogentec S.A. (Belgium). The quadruplex-forming strands (5′-AGG-GTT-AGG-GTT-AGG-GTT-AGG-G-3′) and (5′-GG-GAG-GGT-GGG-GAG-GGT-GGG-3′) were used for human telomeric (HTelo) and *c-myc* studies respectively. For the duplex DNA studies, the 17 base-pair (ds17) complementary strands (5′-CCA-GTT-CGT-AGT-AAC-CC-3′ and 5′-GGG-TTA-CTA-CGA-ACT-GG-3′) and 26 base-pair (ds26) self-complementary strand (5′-CAA-TCG-GAT-CGA-ATT-CGA-TCC-GAT-TG-3′) were used. Calf thymus DNA (ct-DNA) was obtained from Rockland (MB-102-0100). Oligonucleotide concentrations were calculated using the following extinction coefficients (L cm^{-1} mol^{-1}) at 260 nm given by the supplier: 228500 (HTelo), 206800 (c-myc), 253200 (ds26), 160900 (ds17 strand 1), 167400 (ds17 strand 2). The extinction coefficient of ct-DNA at 260 nm was taken to be 13100 L cm^{-1} per mole of nucleotide base pair.[23]

2.2 Syntheses

The synthesis procedures for the substituted salicylaldehyde dibenzyl semicarbazones and their respective copper(II) complexes were adapted from previously-reported methods.[24]

2.2.1 Dibenzyl semicarbazide, $(PhCH_2)_2NCONHNH_2$. Dibenzyl amine (960 μL, 5.0 mmol) was dissolved in dry dichloromethane (8 mL) in a Schlenk tube. Triphosgene (0.519 g, 1.75 mmol) was dissolved in dichloromethane (8 mL) in a separate Schlenk tube and pyridine (810 μL, 10 mmol) was added to this solution. After placing a magnetic stirrer bar into the triphosgene solution, the two flasks were stoppered tightly. The triphosgene solution

was placed in an ice bath on top of a magnetic stirrer. Using a cannula, the amine solution was added dropwise to the triphosgene solution to yield an orange solution. The reaction mixture was left to stand at room temperature for three days under nitrogen to give a yellow solution of dibenzyl carbamic chloride.

To this solution was added diethyl ether (21 mL), and the resultant mixture was added dropwise to a stirred solution of hydrazine monohydrate (970 μL, 20 mmol) in ethanol (10 mL). The reaction mixture was stirred for 30 min before the solvents were removed under reduced pressure. Dichloromethane (5 mL) was added, and the resultant mixture was washed three times with water (5, 3, 3 mL). Evaporation of the organic layer under reduced pressure gave the semicarbazide, which was redissolved in ethanol (1.7 mL) for reaction with the substituted salicylaldehydes. For the synthesis of the 6-OH-substituted semicarbazone, the washed dichloromethane solution was dried with anhydrous sodium sulfate before the solvent was removed, and the semicarbazide residue was redissolved in toluene (5 mL).

2.2.2 Substituted salicylaldehyde dibenzyl semicarbazones. For the salicylaldehyde starting materials that were soluble in toluene (R = 5-Cl, 5-Br, 5-OMe), an equimolar amount of substituted salicylaldehyde dissolved in 4 mL of toluene was added to the solution of the semicarbazide. For the sparingly-soluble salicylaldehydes, 10 mL of toluene was added to the semicarbazide solution, after which the solid salicylaldehyde was added in small portions with vigorous stirring. The resultant mixture was stirred at room temperature for 30 min (12 h for the 6-OH derivative) to give a yellow suspension. A catalytic amount of *p*-toluenesulfonic acid was added if precipitation did not occur within the first 5 min of stirring. The precipitate was isolated by filtration, washed with cold toluene, and dried *in vacuo*. All the semicarbazones were recrystallised from acetone-water mixture.

$C_6H_4(OH)CH=NNHCON(CH_2Ph)_2$. Yield: (1.08 g, 3.01 mmol, 60%). Anal. Calcd. for $C_{22}H_{21}N_3O_2$: C, 73.6; H, 5.9; N, 11.6. Found: C, 73.5; H, 5.9; N, 11.7. IR (cm^{-1}): ν(C=O) 1645 vs. ^{1}H NMR [$(CD_3)_2SO$, ppm]: 11.52 (1H, s, phenol O-H), 10.85 (1H, s, hydrazine N-H), 8.35 (1H, s, imine C-H), 7.2-7.4 (12H, m, Ph-H), 6.88 (2H, m, Ph-H), 4.52 (4H, s, CH_2).

(5-Cl)$C_6H_3(OH)CH=NNHCON(CH_2Ph)_2$. Yield: (1.18 g, 3.00 mmol, 60%). Anal. Calcd. for $C_{22}H_{20}N_3O_2Cl$: C, 67.1; H, 5.1; N, 10.7. Found: C, 66.9; H, 5.3; N, 10.3. IR (cm^{-1}): ν(C=O) 1644 vs. ^{1}H NMR [$(CD_3)_2SO$, ppm]: 11.51 (1H, s, phenol O-H), 10.95 (1H, s, hydrazine N-H), 8.31 (1H, s, imine C-H), 7.2-7.4 (12H, m, Ph-H), 6.90 (1H, d, J= 9.1 Hz, Ph-H), 4.52 (4H, s, CH_2).

(5-Br)$C_6H_3(OH)CH=NNHCON(CH_2Ph)_2$. Yield: (1.38 g, 3.15 mmol, 63%). Anal. Calcd. for $C_{22}H_{20}N_3O_2Br$: C, 60.5; H, 4.5; N, 9.6. Found: C, 60.2; H, 4.2; N, 9.4. IR (cm^{-1}): ν(C=O) 1643 vs. ^{1}H NMR [$(CD_3)_2SO$, ppm]: 11.51 (1H, s, phenol O-H), 10.97 (1H, s, hydrazine N-H), 8.31 (1H, s, imine C-H), 7.2-7.6 (10H, m, Ph-H), 6.96 (2H, d, J= 9.6 Hz, Ph-H), 6.85 (1H, d, J= 8.6 Hz, Ph-H), 4.52 (4H, s, CH_2).

(5-NO_2)$C_6H_3(OH)CH=NNHCON(CH_2Ph)_2$. Yield: (1.25 g, 3.09 mmol, 62%). Anal. Calcd. for $C_{22}H_{20}N_4O_4$: C, 65.3; H, 5.0; N, 13.9. Found: C, 65.0; H, 5.1; N, 13.8. IR (cm^{-1}): ν(C=O) 1651 vs. ^{1}H NMR [$(CD_3)_2SO$, ppm]: 11.10 (1H, s, phenol O-H), 8.45 (2H, s, hydrazine N-H and imine C-H), 8.11 (1H, s, Ph-H), 7.2-7.4 (11H, m, Ph-H), 7.06 (1H, d, J= 10 Hz, Ph-H), 4.52 (4H, s, CH_2).

(5-OMe)$C_6H_3(OH)CH=NNHCON(CH_2Ph)_2$. Yield: (1.03 g, 2.64 mmol, 53%). Anal. Calcd. for $C_{23}H_{23}N_3O_3$: C, 71.0; H, 6.0; N, 10.8. Found: C, 71.0; H, 6.0; N, 11.0. IR (cm^{-1}): ν(C=O)

1645 vs. ^{1}H NMR [$(CD_3)_2SO$, ppm]: 10.90 (1H, s, phenol O-H), 10.81 (1H, s, hydrazine N-H) 8.31 (1H, s, imine C-H), 7.2-7.4 (10H, m, Ph-H), 6.90 (1H, d, J= 2.5 Hz, Ph-H), 6.70-6.80 (2H, m, Ph-H), 4.52 (4H, s, CH_2), 3.70 (3H, s, OCH_3).

$C_{10}H_6(OH)CH=NNHCON(CH_2Ph)_2$. Yield: (1.15 g, 2.81 mmol, 56%). Anal. Calcd. for $C_{26}H_{23}N_3O_2$: C, 76.3; H, 5.6; N, 10.1. Found: C, 76.3; H, 5.7; N, 10.3. IR (cm^{-1}): ν(C=O) 1633 vs. ^{1}H NMR [$(CD_3)_2SO$, ppm]:12.90 (1H, s, phenol O-H), 10.90 (1H, s, hydrazine N-H), 9.20 (1H, s, imine C-H), 8.10 (1H, s, Np-H), 7.86 (2H, m, Np-H), 7.54 (1H, m, Np-H), 7.35 (4H, m, Ph-H), 7.29 (6H, m, Ph-H), 7.20 (2H, m, Np-H), 4.52 (4H, s, CH_2).

(5-OH)C_6H_3(OH)CH=NNHCON($CH_2Ph)_2$. Yield: (1.12 g, 2.98 mmol, 60%). Anal. Calcd. for $C_{22}H_{21}N_3O_3$: C, 70.4; H, 5.6; N, 11.2. Found: C, 70.5; H, 5.5; N, 11.2. IR (cm^{-1}): ν(C=O) 1630 vs. ^{1}H NMR [$(CD_3)_2SO$, ppm]: 10.80 (1H, br s, phenol O-H), 8.95 (1H, br s, phenol O-H), 8.88 (1H, s, hydrazine N-H), 8.27 (1H, s, imine C-H), 7.2-7.4 (10H, m, Ph-H), 6.82 (2H, m, Ph-H), 6.68 (1H, m, Ph-H). 4.52 (4H, s, CH_2).

(3-OH)C_6H_3(OH)CH=NNHCON($CH_2Ph)_2$. Yield: (0.96 g, 2.56 mmol, 51%). Anal. Calcd. for $C_{22}H_{21}N_3O_3$: C, 70.4; H, 5.6; N, 11.2. Found: C, 70.5; H, 5.5; N, 11.2. IR (cm^{-1}): ν(C=O) 1629 vs. ^{1}H NMR [$(CD_3)_2SO$, ppm]: 8.30 (1H, s, imine C-H), 7.2-7.4 (10H, m, Ph-H), 6.80 (2H, m, Ph-H), 6.69 (1H, m, Ph-H), 4.52 (4H, s, CH_2).

(4-OH)C_6H_3(OH)CH=NNHCON($CH_2Ph)_2$. Yield: (1.05 g, 2.80 mmol, 56%). Anal. Calcd. for $C_{22}H_{21}N_3O_3$: C, 70.4; H, 5.6; N, 11.2. Found: C, 70.1; H, 5.7; N, 11.0. IR (cm^{-1}): ν(C=O) 1639 vs. ^{1}H NMR [$(CD_3)_2SO$, ppm]:11.66 (1H, br s, phenol O-H), 10.60 (1H, s, hydrazine N-

H), 9.82 (1H, s, phenol O-H), 8.22 (1H, s, imine C-H), 7.2-7.4 (10H, m, Ph-H), 7.15 (1H, d, J= 9.1 Hz, Ph-H), 6.26-6.32 (2H, m, Ph-H), 4.52 (4H, s, CH_2).

(6-OH)C_6H_3(OH)CH=NNHCON($CH_2Ph)_2$. Yield: (1.08 g, 2.81 mmol, 56%). Anal. Calcd. for $C_{22}H_{21}N_3O_3$. ½ H_2O: C, 68.7; H, 5.7; N, 10.9. Found: C, 68.9; H, 5.7; N, 10.5. IR (cm^{-1}): ν(C=O) 1626 vs. ^{1}H NMR [$(CD_3)_2SO$, ppm]: 11.10 (2H, s, phenol O-H), 10.80 (1H, s, hydrazine N-H), 8.70 (1H, s, imine C-H), 7.2-7.4 (10H, m, Ph-H), 7.0 (1H, m, Ph-H), 6.35 (2H, m, Ph-H), 4.52 (4H, s, CH_2).

2.2.3 Preparation of copper(II) complexes of dibenzyl semicarbazone. Substituted salicylaldehyde dibenzyl semicarbazone (0.50 mmol) was dissolved in 35 mL of dichloromethane. A solution of $CuCl_2.2H_2O$ (0.50 mmol) in methanol (10 mL) was added dropwise to the stirred semicarbazone solution, after which the mixture was stirred for another 15 min. About three-quarters of the solvent was removed under vacuum. Diethyl ether was added dropwise with stirring until a trace amount of precipitate could be seen. After standing at –4 ºC overnight, the precipitate formed was collected by filtration and washed with diethyl ether prior to drying under vacuum.

*Complex **1***. Green colour. Yield: (0.14 g, 0.29 mmol, 58%). Anal. Calcd. for $C_{22}H_{20}ClCuN_3O_2.H_2O$: C, 55.5; H, 4.6; N, 8.8. Found: C, 55.5; H, 4.5; N, 9.0. IR (cm^{-1}): ν(C=O) 1603 vs.

*Complex **2***. Green colour. Yield: (0.16 g, 0.31 mmol, 62%). Anal. Calcd. for $C_{22}H_{19}Cl_2CuN_3O_2.H_2O$: C, 51.8; H, 4.1; N, 8.2. Found: C, 51.8; H, 3.8; N, 8.2. IR (cm^{-1}): ν(C=O) 1606 vs.

*Complex **3***. Green colour. Yield: (0.15 g, 0.28 mmol, 56%). Anal. Calcd. for $C_{22}H_{19}BrClCuN_3O_2$: C, 49.2; H, 3.5; N, 7.8. Found: C, 48.9; H, 3.6; N, 7.6. IR (cm^{-1}): ν(C=O) 1610 vs.

Complex ***4***. Green colour. Yield: (0.14 g, 0.28 mmol, 56%). Anal. Calcd. for $C_{22}H_{19}ClCuN_4O_4$: C, 52.5; H, 3.8; N, 11.1. Found: C, 52.6; H, 3.8; N, 11.2. IR (cm^{-1}): ν(C=O) 1609 vs.

Complex ***5***. Brown colour. Yield: (0.13 g, 0.25 mmol, 50%). Anal. Calcd. for $C_{23}H_{20}ClCuN_3O_3.2H_2O$: C, 52.7; H, 4.4; N, 8.0. Found: C, 52.4; H, 4.3; N, 7.9. IR (cm^{-1}): ν(C=O) 1612 vs.

Complex ***6***. Light green colour. Yield: (0.14 g, 0.28 mmol, 56%). Anal. Calcd. for $C_{26}H_{22}ClCuN_3O_2$: C, 61.5; H, 4.3; N, 8.3. Found: C, 61.5; H, 4.4; N, 8.3. IR (cm^{-1}): ν(C=O) 1603 vs.

Complex ***7***. Brown colour. Yield: (0.18 g, 0.36 mmol, 72%). Anal. Calcd. for $C_{22}H_{20}ClCuN_3O_3.1.75H_2O$: C, 52.3; H, 4.7; N, 8.3. Found: C, 52.0; H, 4.6; N, 8.7. IR (cm^{-1}): ν(C=O) 1603 vs

Complex ***8***. Green colour. Yield: (0.19 g, 0.39 mmol, 78%). Anal. Calcd. for $C_{22}H_{20}ClCuN_3O_3.H_2O$: C, 53.7; H, 4.5; N, 8.6. Found: C, 53.5; H, 4.7; N, 8.6. IR (cm^{-1}): ν(C=O) 1607 vs.

Complex ***9***. Green colour. Yield: (0.15 g, 0.32 mmol, 64%). Anal. Calcd. for $C_{22}H_{20}ClCuN_3O_3$: C, 55.8; H, 4.2; N, 8.9. Found: C, 55.6; H, 4.2; N, 8.5. IR (cm^{-1}): ν(C=O) 1606 vs.

Complex ***10***. Green colour. Yield: (0.12 g, 0.24 mmol, 48%). Anal. Calcd. for $C_{22}H_{20}ClCuN_3O_3.H_2O$: C, 53.4; H, 4.5; N, 8.5. Found: C, 53.4; H, 4.3; N, 8.3. IR (cm^{-1}): ν(C=O) 1611 vs.

2.2.4 Preparation of pyridine derivatives of (dihydroxybenzaldehyde dibenzyl semicarbazone)copper(II) complexes. The corresponding chlorido complex (0.0384 g, 0.081 mmol) was dissolved in 20 mL of methanol in a Schlenk tube. One molar equivalent of silver nitrate (0.0138 g, 0.081 mmol) was added and the solution (shielded from light) was stirred vigorously for 1 h. The resultant mixture was filtered through Celite and evaporated

completely under reduced pressure. Pyridine (10 mL) was added to dissolve the residue, and the solution was stirred at r.t. for 1 h. The dark green solution was evaporated under reduced pressure, and the residue was redissolved in 10 mL of methanol. About 10 mL of diethyl ether was added, and the mixture was stored overnight at 4°C. The precipitate formed was isolated by filtration and washed with diethyl ether.

7-py. Brown colour. Yield: (0.025 g, 0.040 mmol, 50%). Anal. Calcd. for $C_{27}H_{25}CuN_5O_6.2.25\ H_2O$: C, 52.3; H, 4.8; N, 11.3. Found: C, 52.1; H, 4.4; N, 11.1. IR (cm^{-1}): ν(C=O) 1618 vs, ν(NO_3) 1384 vs.

9-py. Green colour. Yield: (0.037 g, 0.064 mmol, 79%). Anal. Calcd. for $C_{27}H_{25}CuN_5O_6$: C, 56.0; H, 4.4; N, 12.1. Found: C, 55.6; H, 4.5; N, 11.7. IR (cm^{-1}): ν(C=O) 1610 vs, ν(NO_3) 1384 vs.

2.3 X-Ray crystallography

Crystals of **9** and **9-py** were grown by slow evaporation of solutions of the complexes in methanol at room temperature. The crystals were mounted on glass fibres for data collection at 298(2)K. The data were collected in the θ/2θ mode using a Siemens P4 diffractometer with Mo Kα radiation (λ = 0.71073 Å), and were corrected for absorption effects using ψ-scan data. The structures were solved by direct methods and refined by full-matrix least-squares on F^2. All non-hydrogen atoms were refined anisotropically. Hydrogen atoms of the molecule were introduced in calculated positions. All hydrogen atoms were allowed to ride on their carrier atoms with idealized bond lengths and angles. Crystal and refinement data and geometric parameters of the crystal structures are given in Table 1.

Table 1 Crystallographic data and structure refinement for compounds **9** and **9-py**.

Compound	9	9-py
Empirical formula	$C_{22}H_{20}ClCuN_3O_3$	$C_{27}H_{25}CuN_5O_6$
Formula weight	473.40	579.06
Crystal system	Triclinic	Monoclinic
Space group	P-1	P2(1)/n
a /Å	9.516(2)	9.587(1)
b / Å	13.668(3)	16.270(2)
c/ Å	17.620(2)	17.130(3)
α(°)	75.658(4)	90
β (°)	84.462(7)	101.44(1)
γ (°)	70.26(2)	90
V/Å3	2089.7(7)	2618.8(6)
Z	4	4
Crystal size/mm	0.30 x 0.20 x 0.10	0.30 x 0.30 x 0.20
Theta range (°)	1.78 to 25.00	2.26 to 25.00
Max. and min. transmission	0.9863 and 0.8699	0.9847 and 0.9042
μ/mm^{-1}	1.202	0.886
Reflns. collected	8742	5931
Independent reflns. (R_{int})	7303 (0.0290)	4618 (0.0208)
R_1, wR_2 [$I > 2\sigma(I)$]	0.0449,0.0919	0.0397, 0.0832

2.4 Fluorescent Intercalator Displacement (FID) Assay[25]

Sample Preparation: The oligonucleotides were dissolved in Milli-Q water to give 100 μM stock solutions. These were diluted in Milli-Q water to give 20 μM solutions, which were further diluted using 10 mM potassium cacodylate (pH 7.4) / 50 mM potassium chloride (60 mM K^+) buffer to give working solutions of 0.50 μM concentration. Prior to use in the FID assay, the DNA strands were annealed by heating to 90 °C for 5 min and cooling to room temperature overnight. The test compounds and thiazole orange (TO) were first dissolved in DMSO to give 1 mM stock solutions, which were then diluted using 10 mM potassium cacodylate (pH 7.4) / 50 mM potassium chloride (60 mM K^+) buffer to give working solutions of various concentrations: 100 μM (test compounds), 3.0 μM (TO for ds26) and 2.5

μM (TO for HTelo, c-myc and ds17). *Procedure*: In a 3-mL quartz cuvette, 750 μL of oligonucleotide solution was mixed with 375 μL of thiazole orange solution. Various volumes of solutions of the test compounds (corresponding to final concentrations of 0 – 2.5 μM) were then added, followed by the appropriate amount of K^+ buffer to bring the total volume to 1.5 mL. After an equilibration time of 3 min, the emission spectrum was recorded between 510 and 750 nm with an excitation wavelength of 501 nm. The fluorescence intensity (peak area) was calculated using the "trapezium rule" method and corrected for the buffer contribution by subtraction. The percentage TO displacement was calculated using the following formula:

$$\%\ \text{TO displacement} = 100 - 100 \times \left[\frac{\text{fluorescence intensity with compound}}{\text{fluorescence intensity without compound}}\right]$$

To accurately determine the DC_{50} value (concentration of test compound causing 50% TO displacement) for compounds that interact strongly with the DNA (DC_{50} < 2.5 μM), the intensity data were plotted using the Stern-Volmer equation,[26] $I_0/I = 1 + kc$, where I_0 = intensity without test compound, I = intensity with test compound, c = concentration of test compound, and k is a constant. Plots of I_0/I against c appear to be linear (Figure S1). When $c = DC_{50}$, $I_0/I = 2$, hence DC_{50} can be obtained from the reciprocal of the gradient of the fitted line (constrained to intercept the vertical axis at 1). The average DC_{50} value was calculated after obtaining three sets of reproducible data within 10 % standard error. For compounds that cause less than 50% TO displacement at 2.5 μM, triplicate measurements of I were made at c = 2.5 μM, and the DC_{50} value was estimated from the two-point (c = 0 and 2.5 μM) Stern-Volmer plot.

2.5 UV-vis spectrophotometric titration

Sample preparation: Solutions of HTelo (2 - 3 mM) and ct-DNA (6 - 10 mM) were prepared by dissolving HTelo and ct-DNA respectively in 50 mM Tris-HCl (pH 7.4) / 100 mM KCl

buffer. The solutions gave ratios of absorbance values at 260 and 280 nm above 1.8:1, indicating that the DNA preparations were free from protein contamination.[27] The copper complexes were first dissolved in DMSO to give 1 mM stock solutions, which were then diluted using 50 mM Tris-HCl (pH 7.4) / 100 mM KCl buffer to obtain 1 mL solutions of 20 μM concentration. *Procedure:* Solutions of the copper complexes were titrated with aliquots (2 μL for HTelo, 10 μL for ct-DNA) of the corresponding DNA solutions until the apparent molar extinction coefficient at the λ_{max} of the complex remained constant for three consecutive additions of the DNA solution. The binding constants (K_b) of the complexes were determined by fitting the data to a plot of [DNA]/(ε_f–ε_a) versus [DNA] using the following equation: [28]

$$[DNA]/(\varepsilon_f-\varepsilon_a) = [DNA]/(\varepsilon_f-\varepsilon_b) + 1/[K_b(\varepsilon_f-\varepsilon_b)]$$

where ε_f and ε_b correspond to the molar extinction coefficients of free and DNA-bound complex respectively, and ε_a is the apparent molar extinction coefficient (absorbance at λ_{max} of complex / concentration of complex).

2.6 Circular Dichroism (CD) Studies

Sample Preparation: HTelo DNA was dissolved in Milli-Q water to give a 100 μM stock solution. The solution was then diluted using 50 mM Tris-HCl /100 mM KCl buffer (pH 7.4) or 50 mM Tris-HCl (pH 7.4) to 5 μM. Prior to use in the CD assay, the DNA solution was annealed by heating the solution to 90 ºC for 5 min, followed by cooling to room temperature overnight. The test compounds were dissolved in DMSO to give 10 mM stock solutions. All solutions were stored at –20 ºC, and were thawed and diluted to 5 mM using DMSO immediately before use. *Procedure*: Measurements were performed with 1:1, 1:2 and 1:4 oligo/compound ratios by adding the appropriate amount of solution of the test compound (5 mM) to 600 μL of the HTelo solution (5 μM) in a strain-free 10 mm × 2 mm rectangular quartz cuvette. After an equilibration time of 5 min, the CD spectra (200-450 nm) were

obtained at 20°C on a JASCO-715 spectrometer using the following parameters: bandwidth, 2 nm; step-size, 0.1 nm; time-pep-point, 4.0 s. The buffer contribution was subtracted manually.

2.7 Cytotoxicity Assay

The cancer cell line, MOLT-4 (human T-lymphoblastic leukaemia), and non-cancerous cell line, IMR-90 (human foetal lung fibroblast), were obtained from the American Type Culture Collection. An RPMI-1640 based medium containing 10 % foetal bovine serum was used to culture MOLT-4 cells, while Eagle's Minimum Essential Medium supplemented with 10 % foetal bovine serum was used for IMR-90 cells. All media also contained 100 units mL^{-1} of penicillin and 100 μg mL^{-1} of streptomycin. The cells were maintained at 37 °C in a 5 % CO_2 incubator.

Cytotoxicity of the compounds was determined using the MTT [3-(3,4-dimethylthiazol-2-yl)-2,5-diphenyltetrazolium bromide] assay[29] on microtitre plates. Both MOLT-4 and IMR-90 cells were seeded at 40,000 cells per well in 70 μL of culture medium. While the suspended MOLT-4 cells were exposed to test compounds immediately after seeding, the adherent IMR-90 cells were cultured for 24 h prior to treatment with compounds.

All compounds were dissolved in absolute DMSO to give 100 mM stock solutions, which were then serially diluted to give working solutions in 10% v/v DMSO in culture medium. Six serial dilutions were made for each compound in order to generate a dose-response curve, and six replicate test wells were set up for each concentration of the compound. Ten microliters of the appropriate working solution was added to each test well, hence the final DMSO concentration was 1.25 % v/v in each well. Each plate also contained a blank well (cell-free medium-only well), solvent control wells which contained cells and 1.25 % v/v

DMSO, drug colour control wells which contained test compound and medium only, and growth control wells which contained only cells in medium.

Following incubation of cells with test compounds for 24 h at 37 °C and 5 % CO_2, 20 μL of a 5 mg mL^{-1} solution of MTT was added to each well (final MTT concentration 1 mg mL^{-1}). Three hours later, 100 μL of lysing solution (20 % sodium dodecyl sulfate dissolved in 50 % *N*,*N*-dimethylformamide, pH adjusted to 4.7 with acetic acid) was added to each well. After the microtitre plate was left to stand overnight, the absorbance of the solution in each well was read at 570 nm. The percent inhibition of growth for each concentration of compound was calculated from the absorbance[29] and plotted against the concentration to give a graph from which the IC_{50} value (concentration of compound required to inhibit the growth of the cells by 50 %) was determined.

2.8 Molecular docking studies

The AutoDock Vina[30] docking software was used to model the binding of complexes **9** and **9-py** with the parallel quadruplex[31] formed from the 22AG HTelo sequence. The crystal structure of the quadruplex was obtained from the Protein Data Bank (PDB code 1KF1). All input structures were prepared from the respective crystal structures using AutoDock Tool (version 1.5.4): the nitrate anion was removed from **9-py**, polar hydrogen atoms were added to the quadruplex structure, and the crystallographic water molecules and non-intercalated potassium ion were removed from the quadruplex. The rotatable bonds of **9** and **9-py** are indicated in yellow in Figure 1.

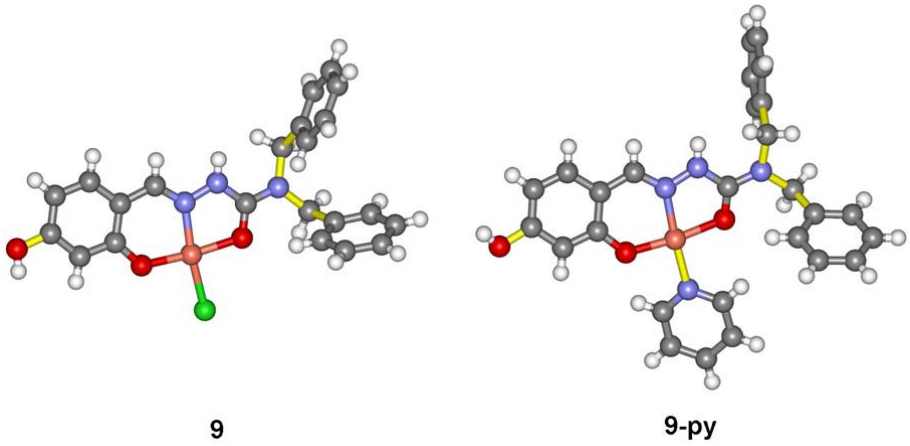

Figure 1. Structures of **9** and **9-py** with rotatable bonds (yellow color).

3 Results and discussion

3.1 Crystal structure of 9

There are two independent molecules of the complex (Figure 2) in the unit cell. These molecules are similar in their gross features, except that the benzyl groups are in *syn* conformation in one molecule and *anti*-conformation in the other. The semicarbazone ligand acts as a tridentate ligand that binds the copper atom via the imine nitrogen [N(1)/N(4)], carbonyl oxygen [O(3)/O(6)] and phenoxo oxygen [O(1)/O(4)] atoms. A chloride ligand occupies the fourth coordination site on each copper atom. The coordination geometry can be described as distorted square planar, with the angles between cis-ligands on each copper atom (Table 2) summing up to 361º. In addition, the three angles about the terminal nitrogen atoms of both the molecules, C(8)-N(3)-C(9), C(8)-N(3)-C(16), C(9)-N(3)-C(16) and C(30)-N(6)-C(38), C(30)-N(6)-C(31), C(31)-N(6)-C(38), sum up to 360º each, indicating a trigonal planar geometry at N(3) and N(6). This implies that the terminal nitrogen atoms are sp^2 hybridised and conjugated with the carbonyl group. Overall, the bond lengths and angles of **9** (Table 2) are in close agreement with those reported for other copper(II) salicylaldehyde semicarbazone complexes.[21, 24]

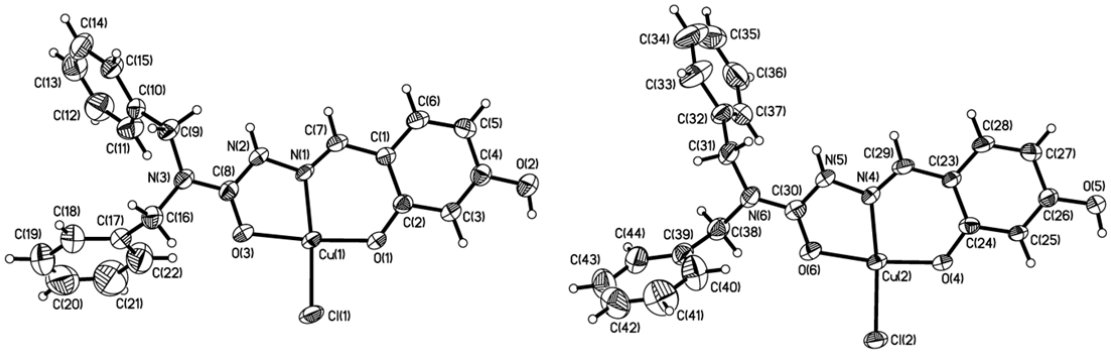

Figure 2. The independent molecules in the crystal structure of **9** (40% probability ellipsoids).

Table 2 Selected bond lengths (Å) and angles (º) for Complexes **9** and **9-py**

Complex 9 (Molecule 1)		**Complex 9 (Molecule 2)**		**Complex 9-py**	
Cu(1)-O(1)	1.897(2)	Cu(2)-O(4)	1.894(2)	Cu(1)-O(1)	1.868(2)
Cu(1)-N(1)	1.935(3)	Cu(2)-N(4)	1.920(3)	Cu(1)-N(1)	1.930(2)
Cu(1)-O(3)	1.957(2)	Cu(2)-O(6)	1.988(3)	Cu(1)-O(3)	1.954(2)
Cu(1)-Cl(1)	2.228(1)	Cu(2)-Cl(2)	2.227(1)	Cu(1)-N(4)	1.979(2)
O(1)-Cu(1)-N(1)	92.7(1)	O(4)-Cu(2)-N(4)	92.6(1)	O(1)-Cu(1)-N(1)	92.75(8)
O(1)-Cu(1)-O(3)	172.4(1)	O(4)-Cu(2)-O(6)	170.7(1)	O(1)-Cu(1)-O(3)	173.32(8)
N(1)-Cu(1)-O(3)	81.0(1)	N(4)-Cu(2)-O(6)	80.8(1)	N(1)-Cu(1)-O(3)	81.38(8)
O(1)-Cu(1)-Cl(1)	95.34(8)	O(4)-Cu(2)-Cl(2)	92.46(7)	O(1)-Cu(1)-N(4)	91.82(9)
N(1)-Cu(1)-Cl(1)	168.93(9)	N(4)-Cu(2)-Cl(2)	173.34(9)	N(1)-Cu(1)-N(4)	173.46(9)
O(3)-Cu(1)-Cl(1)	91.52(8)	O(6)-Cu(2)-Cl(2)	94.68(8)	O(3)-Cu(1)-N(4)	93.78(8)
C(8)-N(3)-C(9)	123.0(3)	C(30)-N(6)-C(31)	123.4(3)	C(8)-N(3)-C(9)	123.0(2)
C(8)-N(3)-C(16)	118.4(3)	C(30)-N(6)-C(38)	120.0(3)	C(8)-N(3)-C(16)	118.8(2)
C(9)-N(3)-C(16)	117.4(3)	C(31)-N(6)-C(38)	116.3(3)	C(9)-N(3)-C(16)	118.0(2)

3.2 Crystal structure of 9-py

The semicarbazone ligand acts as a tridentate ligand that binds the copper atom via the imine nitrogen [N(1)], carbonyl oxygen [O(3)] and phenoxo oxygen [O(1)] atoms. A pyridine ligand occupies the fourth coordination site of the copper atom (Figure 3). There appears to be a very weak interaction between the copper atom and O(6) of the nitrate counterion [Cu(1)···O(6) 2.78 Å]. This interaction has negligible effect on the coordination geometry of the cationic complex, which remains essentially square planar, with the angles between the cis ligands on the copper atom summing up to 360º. As in complex **9**, the three angles about the terminal nitrogen atom, C(8)-N(3)-C(16), C(8)-N(3)-C(9) and C(9)-N(3)-C(16), also sum up to 360º, indicating a trigonal planar geometry and hence conjugation of N(3) with the carbonyl group. The mean plane of the pyridine ring makes an angle of 25.6° with the coordination plane of the copper atom.

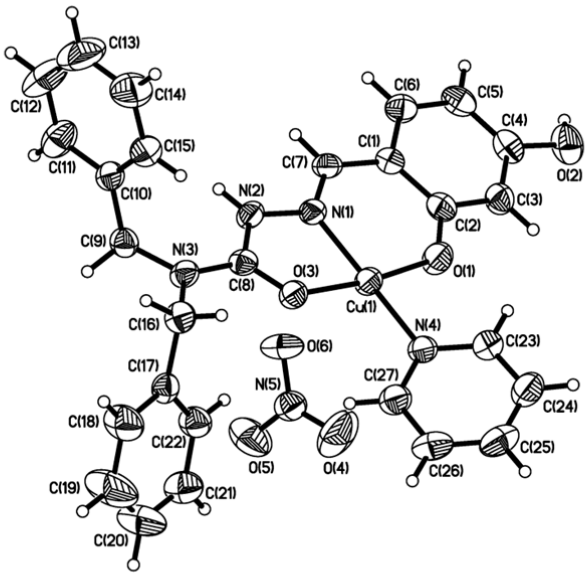

Figure 3. Crystal structure of **9-py** (40% probability ellipsoids).

3.3 Fluorescence Intercalator Displacement assay (FID). The ability of the copper(II) salicylaldehyde semicarbazone complexes to bind to different oligonucleotides via intercalation or end-stacking was evaluated using the FID assay. Two quadruplex forming sequences, HTelo and *c-myc*, and two duplex forming sequences, ds26 and ds17, were used to explore the quadruplex versus duplex selectivity. The DNA affinity is measured by the concentration of the test compound required to displace thiazole orange from the DNA matrix by 50% (DC_{50}), the values of which are given in Table 3.

Table 3 Affinity and selectivity of copper(II) salicylaldehyde semicarbazone complexes for various oligonucleotides, determined by the FID assay.

Complex	DC_{50} (μM) [a]				Selectivity for HTelo [b]		
	HTelo	**c-myc**	**ds17**	**ds26**	***vs.* ds17**	***vs.* ds26**	***vs.* c-myc**
1	20.00 (0.05)	11.1 (0.1)	5.6 (0.1)	12.50 (0.07)	0.28	0.63	0.56
2	9.2 (0.1)	33.2 (0.1)	10.2 (0.2)	16.7 (0.1)	1.1	1.8	3.6
3	15.06 (0.09)	22.7 (0.2)	20.2 (0.1)	28.7 (0.2)	1.34	1.91	1.51
4	39.21 (0.08)	60.0 (0.1)	6.52 (0.08)	16.13 (0.07)	0.17	0.41	1.53
5	33.33 (0.07)	80.6 (0.2)	5.56 (0.06)	11.6 (0.1)	0.18	0.34	2.42
6	22.94 (0.08)	25.6 (0.2)	33.33 (0.08)	14.29 (0.09)	1.45	0.62	1.12
7	2.40 (0.08)	13.32 (0.03)	5.30 (0.05)	13.50 (0.05)	2.21	5.62	5.55
8	26.33 (0.07)	15.3 (0.1)	29.4 (0.1)	15.10 (0.09)	1.12	0.57	0.58
9	2.10 (0.02)	11.22 (0.03)	7.00 (0.06)	4.84 (0.04)	3.33	2.30	5.34
10	15.1 (0.1)	20.7 (0.2)	13.5 (0.1)	20.9 (0.1)	0.90	1.38	1.37
7-py	1.98 (0.03)	10.50 (0.06)	6.50 (0.07)	12.30 (0.06)	3.28	6.21	5.30
9-py	0.55 (0.03)	12.20 (0.05)	5.50 (0.02)	14.3 (0.1)	10	26	22

[a] Standard errors (N = 3) are shown in parentheses. [b] Ratio of DC_{50} for oligonucleotide to DC_{50} for HTelo.

The FID screening showed most of the complexes investigated to have low affinity (DC_{50} > 2.5 μM) for DNA. Amongst the non- and 5-substituted complexes (**1** – **7**), only the hydroxyl-substituted complex **7** shows some affinity for HTelo DNA. Its $^{HTelo}DC_{50}$ value (2.4 μM) is comparable to those of mono-metallic complexes with reasonable binding affinity and selectivity for HTelo DNA.[16-19] This prompted us to study analogous complexes (**8** – **10**) with the hydroxyl group at other positions on the salicylaldehyde ring. Of these, only the 4-hydroxyl analogue, **9**, exhibits some affinity for HTelo. Interestingly, replacement of the chloride ligands of **7** and **9** with pyridine results in an increase in affinity and selectivity for HTelo, especially for the 4-hydroxyl analogue. The increase in affinity is attributed to the presence of a positive charge on **7-py** and **9-py**, which enhances electrostatic binding with the electron-rich guanine groups, and the increase in π surface area for stacking with the G-tetrads. Another interesting feature of complex **9-py** is that it not only displays selectivity for HTelo over duplex DNA, but also over another quadruplex structure, namely c-myc.

3.4 UV-vis Spectrophotometric DNA titration. The binding constants of complexes **7**, **9**, **7-py** and **9-py** towards HTelo and ct-DNA were determined by UV-vis spectrophotometric DNA titration. Addition of HTelo to the complexes resulted in considerable hypochromicity and bathochromic shift of the absorption bands of the complexes. These spectral changes indicate an end-stacking binding mode for the complexes.[32] A typical set of spectra in the presence of increasing amounts of HTelo are shown in Figure 4. The DNA binding constants derived from plots of [DNA]/(ε_f–ε_a) vs. [DNA] are given in Table 4. These data are consistent with the trends in affinity and selectivity observed in the FID assay. It is noteworthy that the $^{HTelo}K_b$ / $^{ct\text{-}DNA}K_b$ ratios of **7-py** and **9-py** exceed that of telomestatin[12] (70) and those of HTelo-selective copper(II)-terpyridine[16] and salphen[19] complexes (2 – 135).

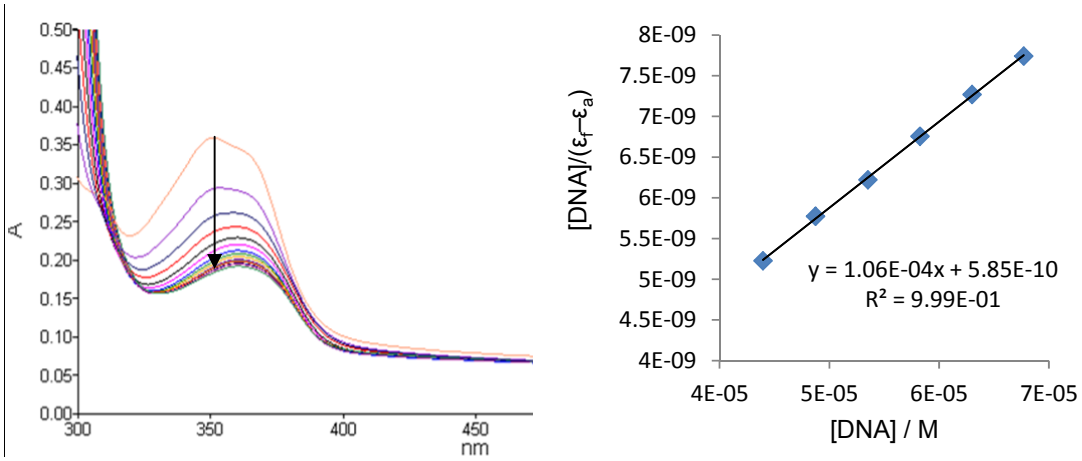

(a) (b)

Figure 4. Titration of complex **9** (20 μM) with HTelo: (a) UV-vis spectral changes with increasing amounts of HTelo; (b) plot of $[DNA]/(\varepsilon_f-\varepsilon_a)$ vs. [DNA].

Table 4 Binding constants, K_b (M^{-1}), of copper(II) salicylaldehyde semicarbazone complexes with HTelo and ct-DNA, determined by UV-vis spectrophotometric titration. Standard errors for K_b values (N = 3) are shown in parentheses.

Complex (λ_{max}/nm)	$^{HTelo}K_b$	$^{ct\text{-}DNA}K_b$	Selectivity [a]
7 (377)	5.77 (0.03) × 10^4	2.79 (0.07) × 10^3	20.7
9 (353)	1.76 (0.05) × 10^5	3.18 (0.05) × 10^3	55.3
7-py (399)	9.46 (0.03) × 10^4	5.55 (0.06) ×10^2	170
9-py (352)	3.42 (0.04) ×10^5	1.62 (0.04) × 10^3	211

[a] Ratio of K_b for HTelo to K_b for ct-DNA.

3.5 Circular Dichroism (CD) Studies. CD spectroscopic studies were carried out to investigate the interaction of complexes **7**, **9**, **7-py** and **9-py** with HTelo. In the presence of potassium ions (100 mM), HTelo adopts a mixture of conformations,[33] as demonstrated by the positive band at 295 nm, the shoulder band between 270-280 nm, and the weaker positive band at 260 nm (Figure 5). A slight decrease in magnitude of molar ellipticity between 230 and 320 nm was typically observed upon addition of increasing amounts of the test compound, although the overall shape of the spectrum was retained (Figure 5). There is

therefore negligible change in the conformation of the HTelo quadruplex when it binds to the copper complexes. The CD spectrum of HTelo in potassium-free buffer showed negligible changes in the presence of the copper complexes (Figure 6). This indicates that the complexes do not template quadruplex formation from the unfolded HTelo sequence. The lack of templating effect of the complexes, despite their selective binding to the HTelo quadruplex in the presence of potassium ions, is consistent with the moderate magnitude of the binding constants. Given that the potassium concentration in cells is in the region of 100 mM, the ability of the complexes to recognize pre-formed quadruplex structures is still biologically relevant.

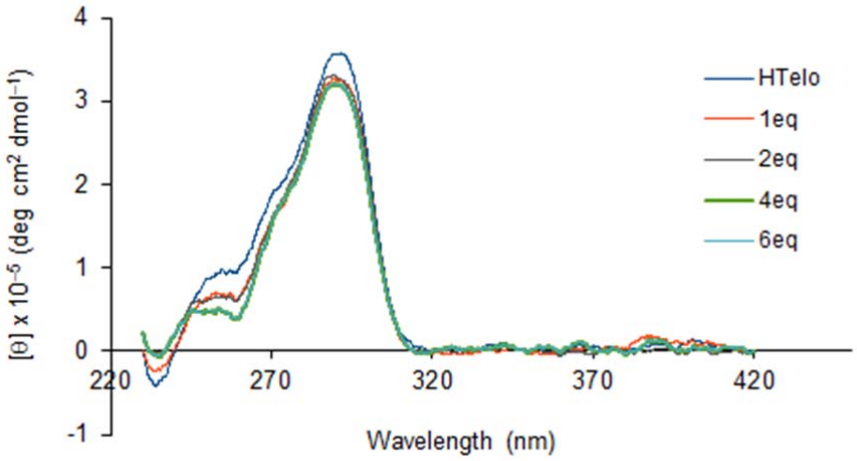

Figure 5. CD spectra of HTelo quadruplex DNA (5 μM) in Tris-HCl 50 mM buffer supplemented with KCl (100 mM) with increasing amounts of complex **7**.

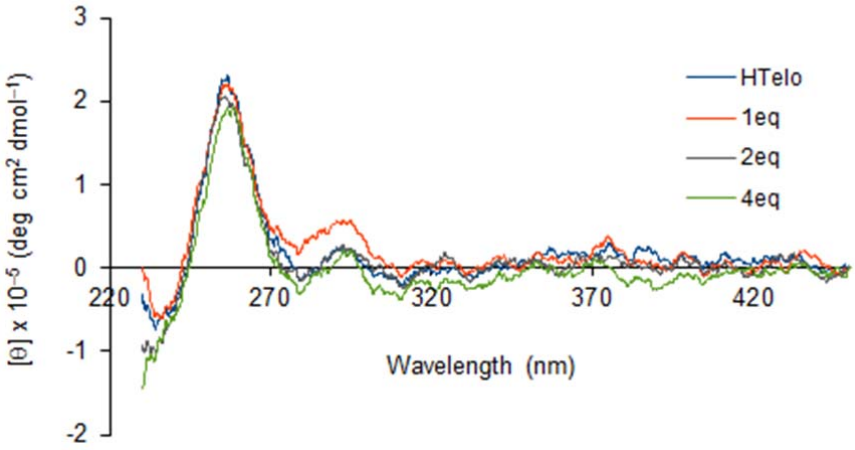

Figure 6. CD spectra of HTelo DNA (5 μM) in 50 mM Tris-HCl buffer (no KCl added) with increasing amounts of complex **7**.

3.6 Molecular docking studies. Molecular docking studies were conducted to investigate the interaction of complexes **9** and **9-py** with the parallel quadruplex[31] formed from the 22AG HTelo sequence. Twenty binding configurations were generated for each complex (Figures S2 and S3). While the majority of these configurations involve the stacking of the complexes on the 3′ or 5′ face of the quadruplex, there are also several configurations wherein the salicylimine moiety occupies one of the channels formed between the TTA loops and G-tetrads. In agreement with the empirical data, the calculated binding affinities (Table 5) indicate that **9-py** binds more strongly than **9** with the quadruplex DNA.

In the most stable binding configuration for **9** (Figure 7), the complex is stacked on the 5′ side of the quadruplex, with its planar core overlapping one of the guanine bases and the benzyl groups being directed into the mouth of a channel formed between the TTA loops and the G-tetrads. The Cu atom is ca. 3.32 Å above the mean plane of the guanine base. A weak hydrogen bond is indicated between the carbonyl oxygen of another guanine base in the tetrad and the 4-OH group of **9** (H···O distance ~2.89Å). Correspondingly, the contribution

of hydrogen bonding to the overall binding affinity is calculated to be –0.27 kcal mol^{-1}. The calculated total hydrophobic contributions to the binding affinity for configurations 1 (described above) and 12 (also stacked, but with benzyl groups pointing away from the quadruplex surface, see Figure S2) are –0.19 and –0.09 kcal mol^{-1}, respectively. This indicates that there are hydrophobic interactions between the benzyl groups and the aforesaid channel in configuration 1.

Table 5. Calculated binding affinity of **9** and **9-py** with DNA G-quadruplex.

Configurations	Binding affinity (kcal mol^{-1})	
	9	**9-py**
1	–6.9	–7.5
2	–6.6	–7.3
3	–6.6	–7.3
4	–6.4	–7.2
5	–6.3	–7.1
6	–6.2	–7.1
7	–6.2	–7.1
8	–6.2	–6.8
9	–6.1	–6.7
10	–6.1	–6.7
11	–6.1	–6.7
12	–6.1	–6.7
13	–6.1	–6.7
14	–5.9	–6.6
15	–5.9	–6.5
16	–5.9	–6.5
17	–5.8	–6.4
18	–5.8	–6.4
19	–5.8	–6.3
20	–5.7	–6.1

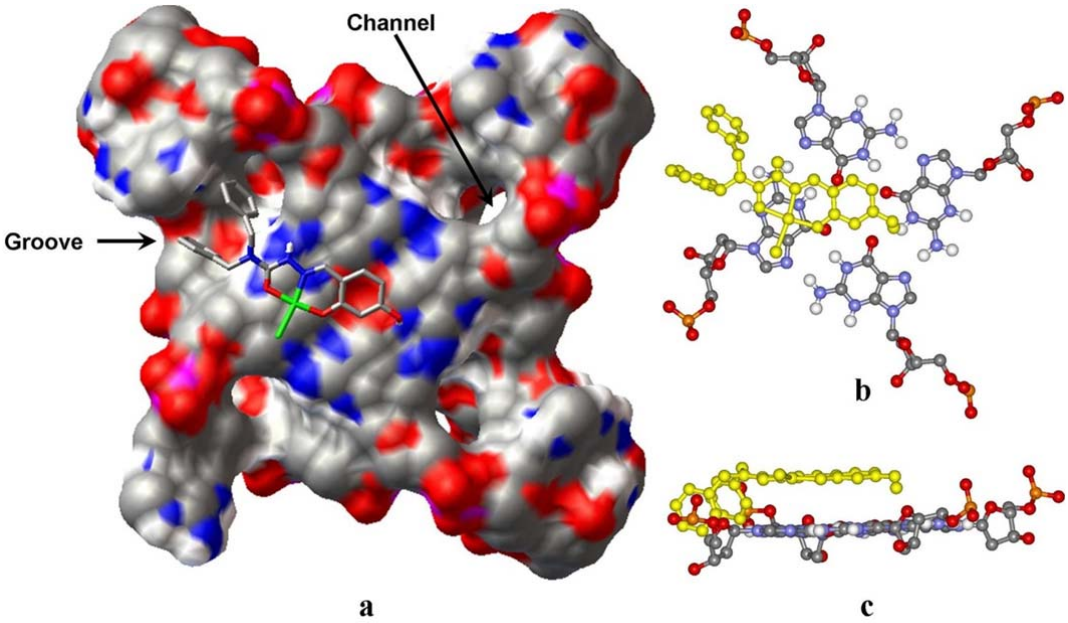

Figure 7. (a) Molecular docking model illustrating the interaction between **9** and DNA G-quadruplex, (b) top and (c) side view of top surface of DNA G-quadruplex containing **9**.

Complex **9-py** is also 5′-stacked with its benzyl groups inside a channel in its most favoured configuration (Figure 8). The pyridine ring overlaps the imidazole ring of a guanine base, with a centroid (pyridine) – mean plane (guanine) distance of ca. 3.63 Å. As in the case of **9**, a weak hydrogen bond (albeit stronger than that for **9**) exists between a guanine carbonyl oxygen and the 4-OH group of **9-py** (H···O distance ~2.39Å). The calculated hydrogen bonding contribution to the binding affinity is –0.40 kcal mol^{-1}.

In summary, the docking results indicate that the higher HTelo affinity of **9-py** is due to the additional π–π interaction afforded by the pyridine ring, and stronger hydrogen bonding with the guanine oxygen. The results also suggest that it may be possible to enhance the interaction of the copper complex with the channel and/or groove of the HTelo quadruplex by functionalizing the benzyl groups and/or pyridine ring of **9-py**. This may result in new complexes with higher affinity and selectivity for HTelo.

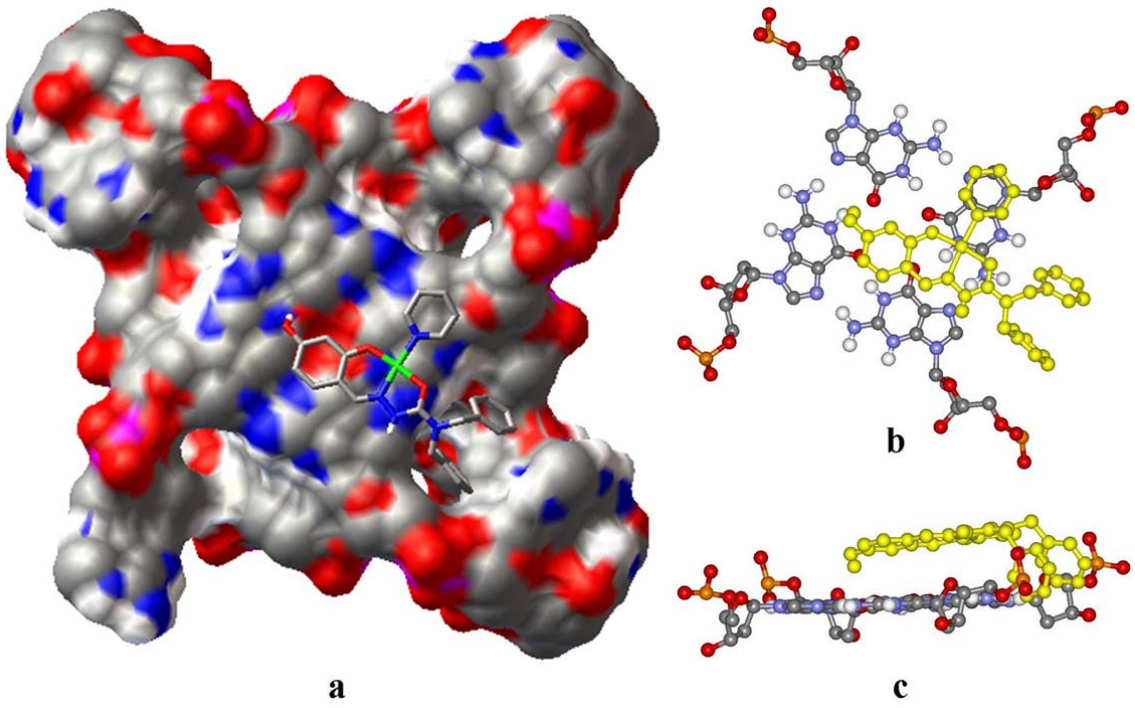

Figure 8. (a) Molecular docking model illustrating the interaction between **9-py** and DNA G-quadruplex, (b) top and (c) side view of top surface of DNA G-quadruplex containing **9-py**.

3.7 Cytotoxicity. Most of the copper(II) salicylaldehyde semicarbazone complexes tested show high cytotoxicity against MOLT-4 human leukaemia cells, with IC_{50} values in the low micromolar region (Table 6). In addition, these complexes inhibit MOLT-4 cells selectively over non-cancerous IMR-90 human fibroblasts, especially for **9-py**. It is also noteworthy that, whilst **7-py** is not exceptional in its toxicity towards MOLT-4 cells, it has negligible toxicity towards the fibroblasts. Interestingly, there is good correlation between the selectivity for MOLT-4 cells and that for HTelo amongst the complexes that bind more strongly to HTelo (Table 6). This might indicate that the mode of action of these complexes involve their binding to telomeric DNA. Generation of DNA-cleaving reactive oxygen species may occur after DNA binding, leading to cell death. The ability of copper(II) salicylaldehyde semicarbazone complexes to cleave DNA via the generation of reactive oxygen species has been documented.[22]

On the whole, the complexes with low affinity for HTelo appear to be more active than their stronger-binding counterparts against both MOLT-4 and IMR-90 cells. The weakly-binding complexes are unlikely to act via interaction with telomeric DNA, however. Correspondingly, there is no discernible correlation between their selectivity for HTelo and their selectivity for MOLT-4 cells. Mediation of oxidative damage might be the dominant mode of action instead for these complexes.

Table 6 Cytotoxicity and selectivity of copper(II) salicylaldehyde semicarbazone complexes against MOLT-4 and IMR-90 cells. Standard errors for IC_{50} values (N = 6) are given in parentheses. Selectivity values of the complexes between HTelo and ds26 oligonucleotides are included for comparison.

Complex	IC_{50} (μM)		Selectivity	
	MOLT-4	IMR-90	$^{IMR\text{-}90}IC_{50}$ / $^{MOLT\text{-}4}IC_{50}$	$^{ds26}DC_{50}$ / $^{HTelo}DC_{50}$
Strong HTelo binders				
9-py	3.1 (0.2)	30.2 (0.4)	9.7	26
7-py	18.1 (0.5)	> 125	> 6.9	6.2
7	5.0 (0.2)	31.5 (0.5)	6.3	5.6
9	8.03 (0.08)	30.5 (0.8)	3.8	2.3
Weak HTelo binders				
6	1.0 (0.4)	11.7 (0.5)	12	0.62
4	1.1 (0.1)	7.3 (0.8)	6.6	0.41
8	1.93 (0.08)	10.3 (0.5)	5.3	0.57
1	2.1 (0.3)	7.3 (0.1)	3.5	0.63
5	1.9 (0.1)	5.03 (0.08)	2.6	0.34
10	15.3 (0.4)	30.1 (0.2)	2.0	1.4
2	5.5 (0.3)	6.8 (0.4)	1.2	1.8
3	5.9 (0.2)	6.8 (0.4)	1.2	1.9

4 Summary and Conclusion

A series of copper(II) complexes containing substituted salicylaldehyde dibenzyl semicarbazone ligands have been prepared. Amongst the chloridocopper(II) complexes, only those of the 4- and 5-hydroxyl-substituted ligands (complexes **9** and **7**) show affinity for HTelo quadruplex DNA. Complexes **7** and **9** also show good selectivity for HTelo over c-myc and duplex DNA. The chlorido ligands of **7** and **9** can be substituted with pyridine, yielding derivatives (**7-py** and **9-py**) with improved affinity and much higher selectivity for HTelo DNA. Molecular docking studies show that **9** and **9-py** stack on the G-tetrad at the 5′-end of the HTelo quadruplex, with the benzyl groups directed into a channel formed between the TTA loops and the G-tetrads, and the hydroxyl group forming a hydrogen bond with a guanine residue. Most of the complexes prepared in this work show high cytotoxicity against MOLT-4 human leukaemia cells. Complexes **7**, **9**, **7-py** and **9-py** also exhibit high selectivity for MOLT-4 cells over non-cancerous IMR-90 human fibroblasts.

5 Acknowledgements

Financial support from the National Institute of Education, Singapore (grants RS 12/10 YYK and RI 10/10 PL) and from the Engineering and Physical Sciences Research Council, UK are gratefully acknowledged. The authors also thank Ms Ying-Chang Ting, Hui-Xin Ting, and Wan-Yen Lee for technical assistance.

6 Supplementary Information

Crystallographic data (excluding structure factors) for complexes **9** and **9-py** may be obtained from the Cambridge Crystallographic Data Centre (CCDC, 12 Union Road, Cambridge CB2 1EZ, UK; fax: _/44-1223-336-033; e-mail: deposit@ccdc.cam.ac.uk or www:

http://www.ccdc.cam.ac.uk) on quoting the depository numbers CCDC 955520 and 955521, respectively.

REFERENCES

1. Burge, S.; Parkinson, G. N.; Hazel, P.; Todd, A. K.; Neidle, S. *Nucleic Acids Res*. **2006,** *34*, 5402.

2. Parkinson, G. N.; Cuenca, F.; Neidle, S. *J Mol.Bio.* **2008**, *381*,1145.

3. Neidle, S.; Parkinson, G. N. *Biochimie*. **2008**, *90*, 1184.

4. Jiang, Y. L.; Liu, Z. P. *Mini Rev. Med. Chem*. **2010**, *10*, 726.

5. Blasco, M. A. *Eur. J. Cell Biol*. **2003**, *82*, 441.

6. De Cian, A.; Lacroix, L.; Douarre, C.; Temime-Smaali, N.; Trentesaux, C.; Riou, J. F.; Mergny, J. L. *Biochimie*. **2008**, *90*, 131.

7. Rangan, A.; Fedoroff, O. Y.; Hurley, L. H. *J. Biol. Chem*. **2001**, *276*, 4640.

8. Siddiqui-Jain, A.; Grand, C. L.; Bearss, D. J.; Hurley, L. H. *Proc. Natl. Acad. Sci. U. S. A*. **2002**, *99*, 11593.

9. Fernando, H.; Reszka, A. P.; Huppert, J.; Ladame, S.; Rankin, S.; Venkitaraman, A. R.; Neidle, S.; Balasubramanian, S. *Biochemistry.* **2006**, *45*, 7854.

10. Rankin, S.; Reszka, A. P.; Huppert, J.; Zloh, M.; Parkinson, G. N.;Todd, A. K.; Ladame, S.; Balasubramanian, S.; Neidle, S. *J. Am. Chem. Soc*. **2005**, *127*, 10584.

11. Qin, Y.; Hurley, L. H. *Biochimie*. **2008**, *90*, 1149.

12. Monchaud, D.; Teulade-Fichou, M.-P. *Org. Biomol. Chem*. **2008**, *6*, 627.

13. Ou, T.-M.; Lu, Y.-J.; Tan, J.-H.; Huang, Z.-S.; Wong, K.-Y.; Gu, L.-Q. *ChemMedChem* **2008**, *3*, 690.

14. Reed, J. E.; White, A. J. P.; Neidle, S.; Vilar, R. *Dalton Trans*. **2009**, 2558.

15. Barry, N. P. E.; Abd Karim, N. H.; Vilar, R.; Therrien, B. *Dalton Trans*. **2009**, 10717.

16. Suntharalingam, K.; White, A. J. P.; Vilar, R. *Inorg. Chem*. **2010**, *49*, 8371.

17. Suntharalingam, K.; Gupta, D.; Sanz Miguel, P.J.; Lippert, B,; Vilar, R. Chem.Eur. J. **2010,** *16*, 3613.

18. Georgiades, S. N.; Abd Karim, N. H.; Suntharalingam, K.; Vilar, R. *Angew. Chem. Int. Ed.* **2010**, *49*, 4020.

19. Campbell, N. H.; Abd Karim, N. H.; Parkinson, G. N.; Gunaratnam, M.; Petrucci, V.; Todd, A.K.; Vilar, R.; Neidle, S. *J. Med. Chem*. **2012**, *55*, 209.

20. von Grebe, P.; Suntharalingam, K.; Vilar, R.; Sanz Miguel, P. J.; Herres-Pawlis, S.; Lippert, B. *Chem. Eur. J.* **2013**, *19*, 11429.

21. Lee, W. Y.; Lee, P. P. F.; Yan, Y. K.; Lau, M. *Metallomics*. **2010**, *2*, 694.

22. Lee, W. Y.; Yan, Y. K.; Lee, P. P. F.; Tan, S. J.; Lim, K. H. *Metallomics*. **2012**, *4*, 188.

23. Bresloff, J. L.; Crothers, D. M. *Biochemistry* **1981**, *20*, 3547.

24. Lee, P. F.; Yang, C. T.; Fan, D.; Vittal, J. J.; Ranford. J. D. *Polyhedron*. **2003**, *22*, 2781.

25. Monchaud, D.; Allain, C.; Bertrand, H.; Smargiasso, N.; Rosu, F.; Gabelica, V.; De Cian, A,; Mergny, J. L.; Teulade-Fichou, M. P. *Biochimie*. **2008**, *90*, 1207.

26. Li, Y.; Yang, Z. Y. *Inorg. Chim. Acta* **2009**, *362*, 4823.

27. Marmur, J., *J. Mol. Biol.*, 1961, **3**, 208.

28. Kumar, C. V. and Asuncion, E. H., *J. Am. Chem. Soc*., **1993**, *115*, 8547.

29. Hansen, M. B.; Nielsen, S. E.; Berg, K. *J. Immunol. Methods*, **1989**, *119*, 203.

30. Trott, O.; Olson, A. J. *J. Comput. Chem.* **2010**, *31*, 455.

31. Parkinson, G. N.; Lee, M. P. H.; Neidle, S. *Nature*, **2002**, *417*, 876.

32. Long, E. C.; Barton, J. K. *Acc. Chem. Res.* **1990**, *23*, 271.

33. Masiero, S.; Trotta, R.; Pieraccini, S.; Tito, S, D.; Perone, R.; Randazzo, A.; Spada, G, P. *Org. Biomol. Chem.* **2010**, 8, 2683.

Copper(II) Complexes of Substituted Salicylaldehyde Dibenzyl Semicarbazones: Synthesis, Cytotoxicity and Interaction with Quadruplex DNA

Siti Munira Haidad Ali[a], Yaw-Kai Yan[a,*], Peter P. F. Lee[a], Kenny Zhi Xiang Khong[a], Mahasin Alam Sk[b], Kok Hwa Lim[b], Beata Klejevskaja[c], Ramon Vilar[c],

Supplementary Figures

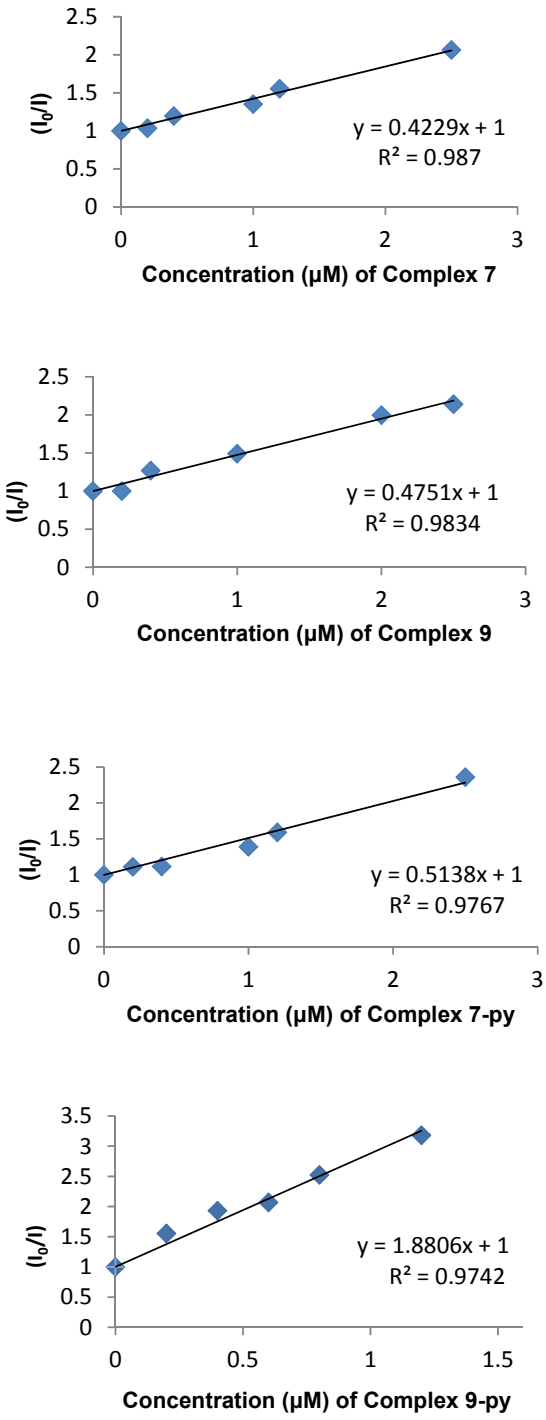

Figure S1. Stern-Volmer plots for complexes **7**, **9**, **7-py** and **9-py**.

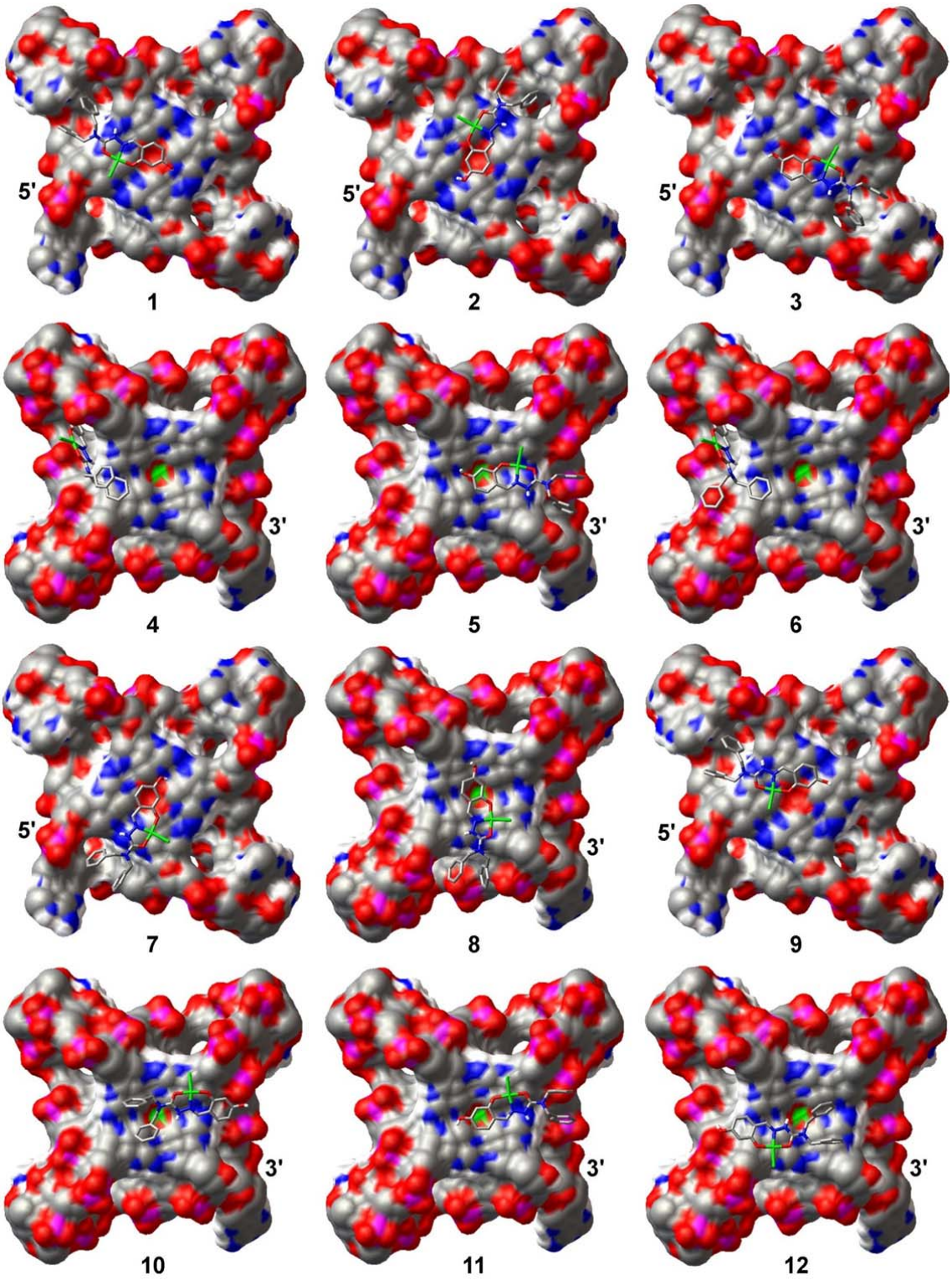

Figure S2. Molecular docking configurations of complex **9** with the 22AG quadruplex.
Figure S2 continues on the next page.

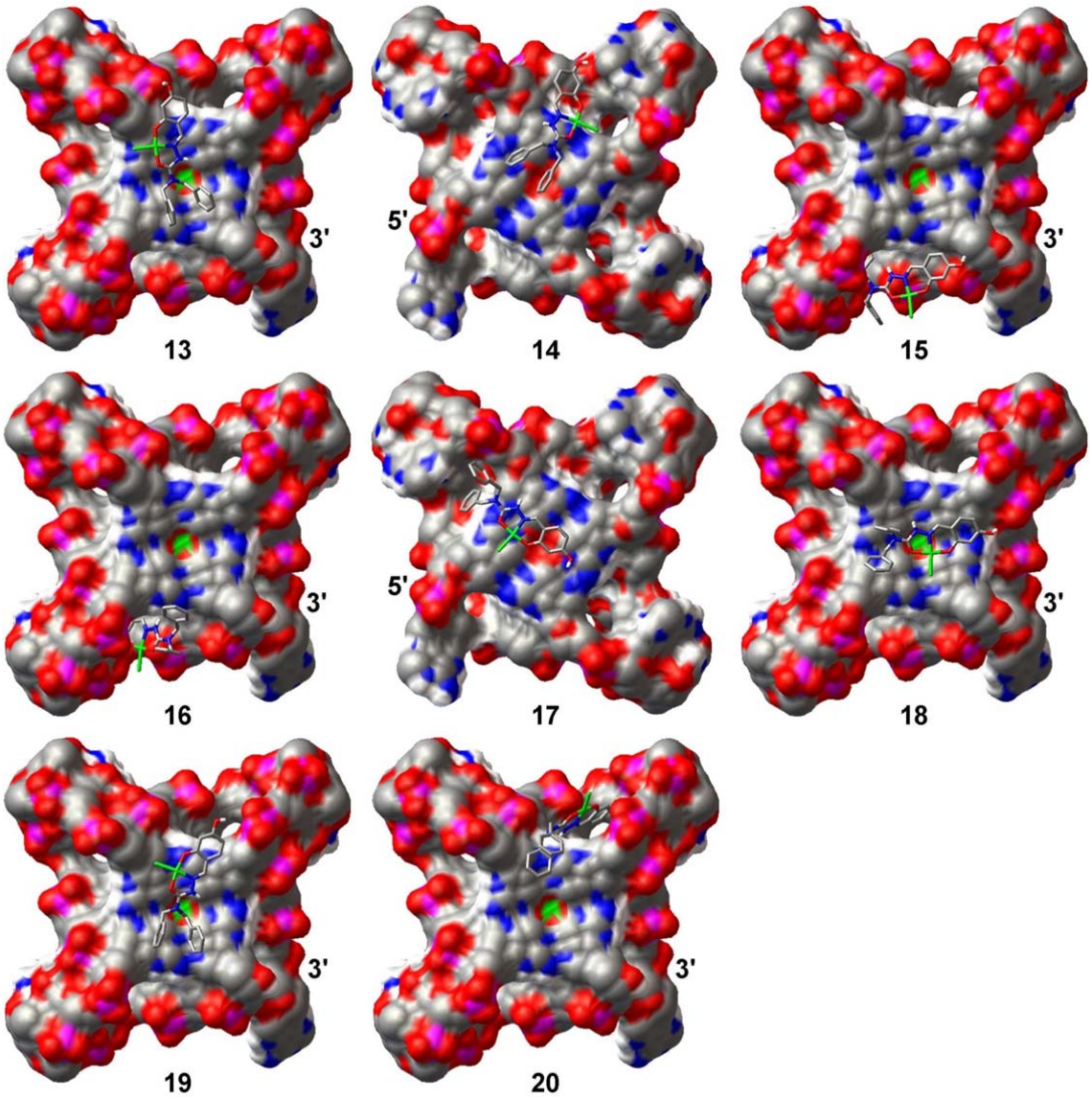

Figure S2 (cont'd). Molecular docking configurations of complex **9** with the 22AG quadruplex.

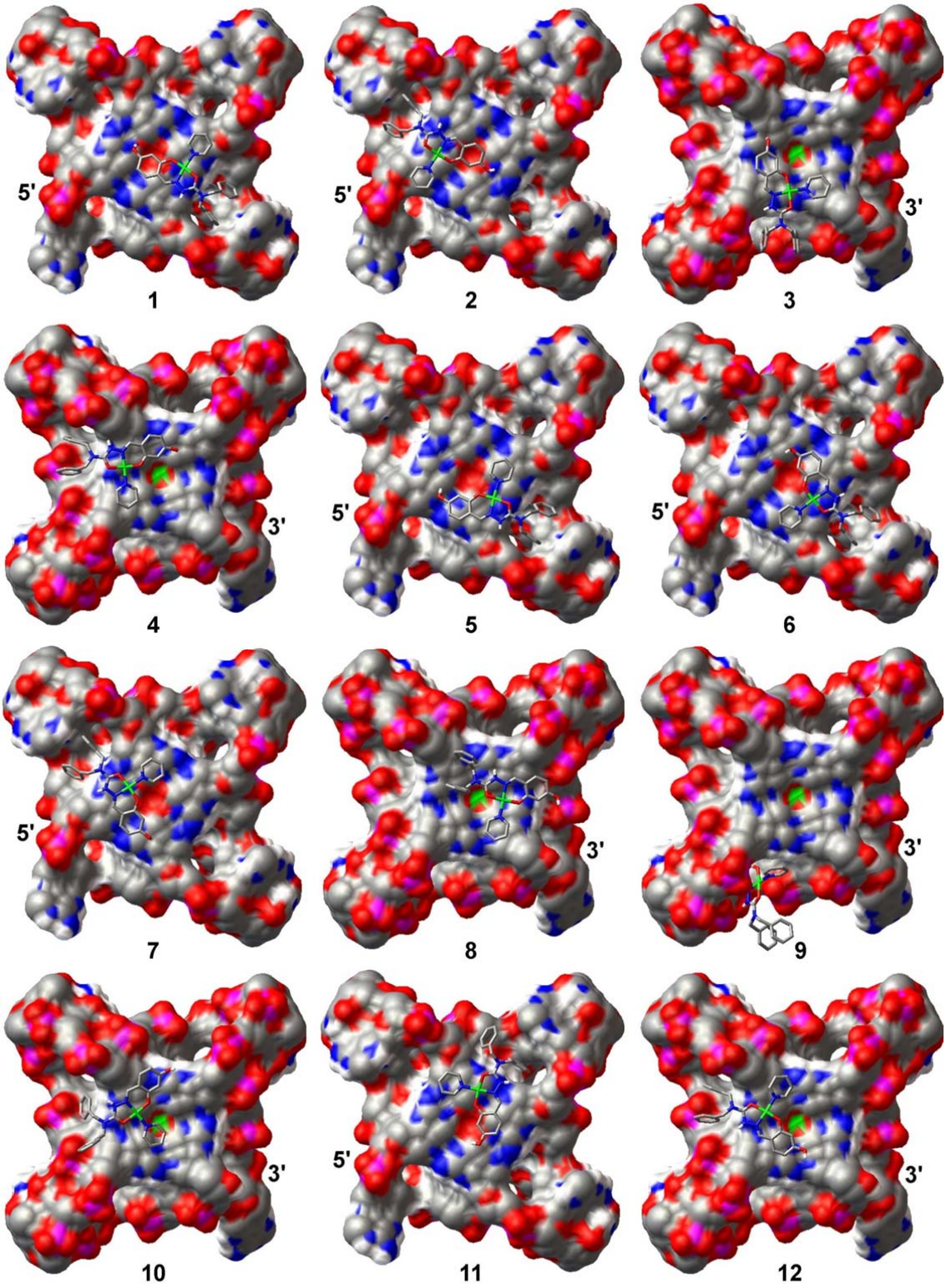

Figure S3. Molecular docking configurations of complex **9-py** with the 22AG quadruplex. Figure S3 continues on the next page.

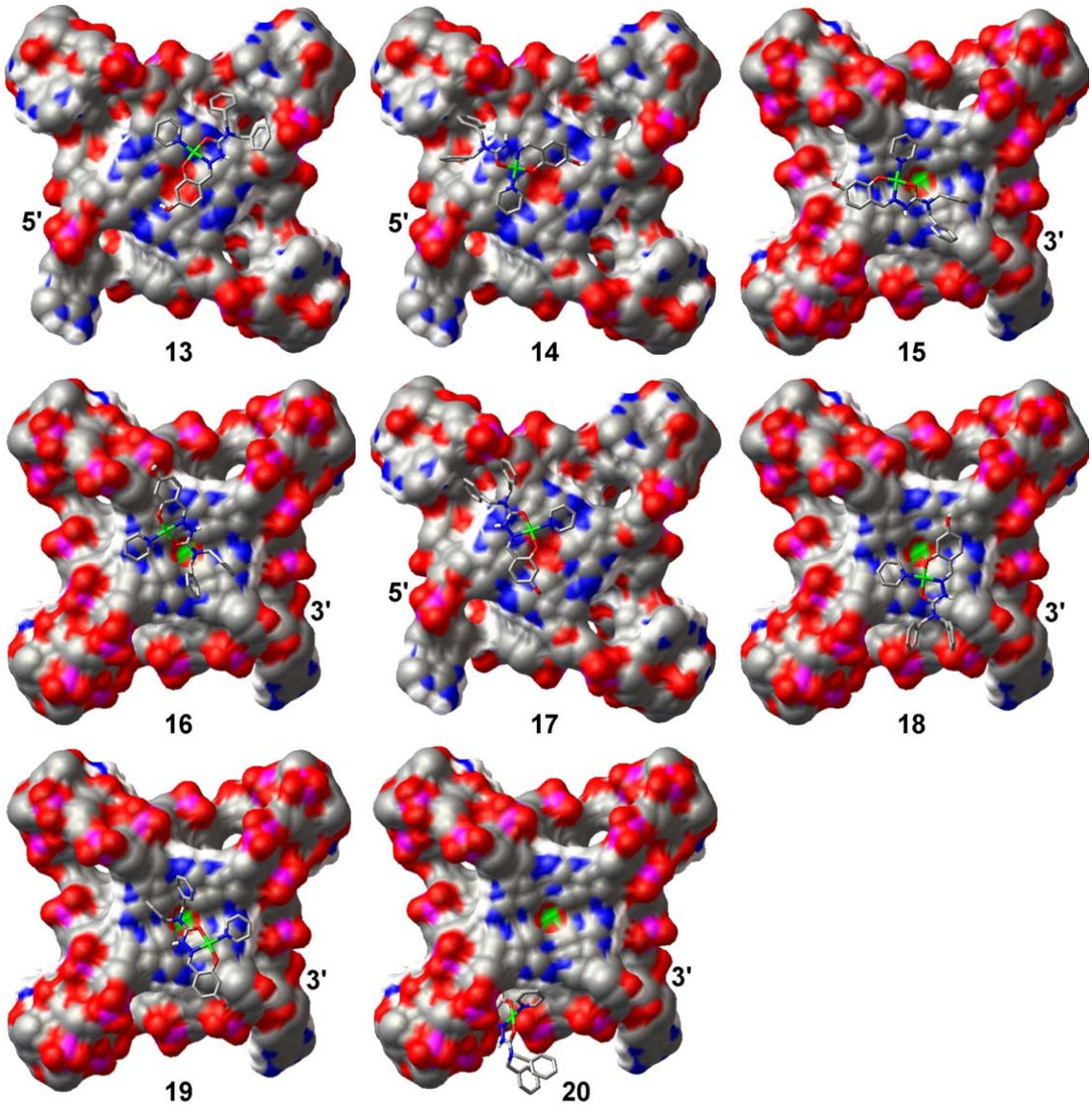

Figure S3 (cont'd). Molecular docking configurations of complex **9-py** with the 22AG quadruplex.